arXiv:cond-mat/0311181v4 [cond-mat.supr-con] 24 Feb 2004

$CePt_3Si$: an unconventional superconductor without inversion center

K. V. Samokhin, E. S. Zijlstra, S. K. Bose
Department of Physics, Brock University, St.Catharines, Ontario, Canada L2S 3A1
(Dated: March 22, 2022)

Most superconducting materials have an inversion center in their crystal lattices. One of few exceptions is the recently discovered heavy-fermion superconductor $CePt_3Si$ [E. Bauer *et al*, Phys. Rev. Lett. **92**, 027003 (2004)]. In this paper, we analyze the implications of the lack of inversion symmetry for the superconducting pairing. We show that the order parameter is an odd function of momentum, and that there always are lines of zeros in the excitation energy gap for one-component order parameters, which seems to agree with the experimental data. The superconducting phase can be non-uniform, even without external magnetic field, due to the presence of unusual gradient terms in the Ginzburg-Landau free energy. Also, we performed *ab initio* electronic structure calculations for $CePt_3Si$, which showed that the spin-orbit coupling in this material is strong, and the degeneracy of the bands is lifted everywhere except along some high symmetry lines in the Brillouin zone.

PACS numbers: 74.20.Rp, 74.70.Tx, 71.20.Be

I. INTRODUCTION

In the past two decades, a number of novel superconducting materials have been discovered where order parameter symmetries are different from an s-wave spin singlet, predicted by the Bardeen-Cooper-Schrieffer (BCS) theory of electron-phonon mediated pairing. From the initial discoveries of unconventional superconductivity in heavy-fermion compounds, the list of examples has now grown to include the high-T_c cuprate superconductors, ruthenates, ferromagnetic superconductors, and possibly organic materials. In most of these materials, there are strong indications that the pairing is caused by the electron correlations, in contrast to conventional superconductors such as Pb, Nb, *etc*. Non-phononic mechanisms of pairing are believed to favor a non-trivial spin structure and orbital symmetry of the Cooper pairs. For example, the order parameter in the high-T_c superconductors, where the pairing is thought to be caused by the anti-ferromagnetic correlations, has the d-wave symmetry with lines of zeroes at the Fermi surface.

A powerful tool of studying unconventional superconducting states is symmetry analysis, which works even if the pairing mechanism is not known. Mathematically, superconductivity is a consequence of the breaking of the gauge symmetry $U(1)$ in the full symmetry group of the normal state: $\mathcal{G} = S_M \times U(1)$, where S_M is a magnetic space group, which includes usual space group operations (i.e. translations, rotations, inversion, *etc*) and time reversal operation K. In a non-magnetic crystal, $S_M = S \times \mathcal{K}$, where S is the space group, and $\mathcal{K} = \{E, K\}$. In a magnetic crystal, K enters S_M only in combination with other symmetry elements. The superconducting state is said to be "unconventional" if, in addition to the gauge symmetry, some other symmetries from $\mathcal{G}$ are broken. The group-theoretical analysis of unconventional superconducting states in non-magnetic crystals was developed in Refs. [1, 2]. Recently, it was extended to include the ferromagnetic case [3, 4, 5].

In almost all previous studies, it was assumed that the crystal has an inversion center, which leads to degenerate electron bands and makes it possible to classify the Cooper pair states according to their spin (or pseudospin if the spin-orbit coupling is taken into account). The even (singlet) and odd (triplet) components of the superconducting order parameter can then be studied separately [6]. Although this is the case in most superconductors, there are some exceptions. Early discussion of the possible loss of inversion symmetry associated with a structural phase transition in V_3Si, which is an A15 type superconductor, can be found in Ref. [7]. Later, a C15 superconductor HfV_2 was found to undergo a transition from a cubic to a non-centrosymmetric body-centered orthorhombic structure [8]. The possible existence of superconductivity was reported in ferroelectric perovskite compounds $SrTiO_3$ [9] and $BaPbO_3$-$BaBiO_3$ [10]. More recently, there has been a renewed theoretical interest in this problem, mainly in the context of superconductivity in two-dimensional (2D) systems, such as Cu-O layers in YBCO [11], or surface superconductivity on Tamm levels [12, 13]. According to Ref. [11, 12], in the absence of inversion symmetry the order parameter becomes a mixture of spin-singlet and spin-triplet components, which leads, for instance, to the Knight shift attaining a nonzero value at $T = 0$. Other peculiar properties of noncentrosymmetric superconductors include a jump of magnetic induction at the surface [14], and the possibility of non-uniform helical superconducting phases due to the presence of first-order gradient terms in the Ginzburg-Landau (GL) functional [15].

This work is motivated by a recent experimental discovery of superconductivity with $T_c \simeq 0.75K$ in $CePt_3Si$ [16], which is the first known heavy-fermion material without inversion center. (It should be mentioned that incommensurate density modulations might break inversion symmetry in a heavy-fermion compound UPt_3, as pointed out in Ref. [17].) Our goal is two-fold. First, we study the symmetry of electron bands, calculate the electronic structure, and estimate the magnitude of the spin-orbit coupling in the normal state of $CePt_3Si$. Second, we

use general symmetry arguments to analyze the gap symmetry and spatial dependence of the order parameter in a three-dimensional non-centrosymmetric tetragonal superconductor, assuming a strong spin-orbit coupling and the clean limit. The paper is organized as follows. In Sec. II, we study symmetry of the single electron states. In Sec. III, the results of the electronic band structure calculations are reported. Sec. IV focuses on the symmetry of the superconducting order parameter, possible locations of the gap nodes, and also spatial structure of the superconducting phase, using the phenomenological Ginzburg-Landau approach. Sec. V concludes with a discussion of our results.

II. SYMMETRY OF ELECTRON BANDS

The symmetry group of the normal paramagnetic state: $\mathcal{G} = S \times \mathcal{K} \times U(1)$, where S is the space group of the crystal, and $U(1)$ is the gauge group. In the case of $CePt_3Si$, the space group is P4mm (No. 99), which is generated by (i) lattice translations by the primitive vectors $\boldsymbol{a} = a(1,0,0)$, $\boldsymbol{b} = a(0,1,0)$, $\boldsymbol{c} = c(0,0,1)$ of a tetragonal lattice, and (ii) the generators of the point group $G = \mathbf{C}_{4v}$: the rotations C_{4z} about the z axis by an angle $\pi/2$ and the reflections σ_x in the vertical plane (100). Spatial inversion I is not an element of the symmetry group.

In the absence of inversion symmetry, spin-orbit (SO) coupling plays a crucial role due to its band-splitting effect. At non-zero SO coupling, the single-particle wavefunctions are linear combinations of the eigenstates of the spin operator s_z: $\langle \boldsymbol{r}|\psi\rangle = u(\boldsymbol{r})\chi_\uparrow + v(\boldsymbol{r})\chi_\downarrow$. Since the normal state Hamiltonian H_0 is invariant with respect to the crystal lattice translations, the eigenfunctions are the Bloch spinors $\psi_{\boldsymbol{k},n}(\boldsymbol{r})$ belonging to the wave vectors $\boldsymbol{k}$ in the Brillouin zone, which can be written in the form

$$\langle \boldsymbol{r}|\boldsymbol{k},n\rangle = u_{\boldsymbol{k},n}(\boldsymbol{r})\chi_\uparrow + v_{\boldsymbol{k},n}(\boldsymbol{r})\chi_\downarrow. \qquad (1)$$

The corresponding eigenvalues $\epsilon_n(\boldsymbol{k})$ describe the band dispersion of free electrons.

In the presence of both the time-reversal and inversion symmetries the bands are two-fold degenerate at each $\boldsymbol{k}$. Indeed, the states $|\boldsymbol{k},n\rangle$ and $KI|\boldsymbol{k},n\rangle$ correspond to the same $\boldsymbol{k}$, have the same energy, and are orthogonal (in addition, these two states are degenerate with another pair of orthogonal states, $K|\boldsymbol{k},n\rangle$ and $I|\boldsymbol{k},n\rangle$, which correspond to $-\boldsymbol{k}$). In this case, $n = (\nu,\pm)$, where $\pm$ labels the linearly independent Bloch states at a given band index ν. There is a freedom in choosing the basis functions $|\boldsymbol{k},\nu,+\rangle$ and $|\boldsymbol{k},\nu,-\rangle$. The most frequently used convention is that they should transform under rotations R similar to the spin eigenstates $|\boldsymbol{k},\nu,\uparrow\rangle$ and $|\boldsymbol{k},\nu,\downarrow\rangle$, i.e.

$$R|\boldsymbol{k},\nu,\alpha\rangle = U_{\alpha\beta}(R)|R\boldsymbol{k},\nu,\beta\rangle, \qquad (2)$$

where $\alpha,\beta = \pm$ and $U(R)$ is the spin-rotation matrix: for a rotation by an angle θ around some axis $\boldsymbol{n}$: $U(R) = \exp[-i(\theta/2)(\boldsymbol{\sigma}\cdot\boldsymbol{n})]$ ($\boldsymbol{\sigma}$ are Pauli matrices). The practical recipe for constructing the basis of the Bloch states is as follows: first choose a state $|\boldsymbol{k},\nu,+\rangle$ at each $\boldsymbol{k}$ in the irreducible part of the first Brillouin zone, then act on it by KI to obtain an orthogonal state $|\boldsymbol{k},\nu,-\rangle$ at the same $\boldsymbol{k}$, and finally act on $|\boldsymbol{k},\nu,\pm\rangle$ by the elements of the point group and use the prescription (2) to obtain the pairs of the basis functions belonging to the star of $\boldsymbol{k}$. The single-electron states constructed in this way are referred to as the pseudospin states [2]. It is the presence of the inversion center that makes the bands double degenerate in a non-magnetic crystal: $\epsilon_{\nu,+}(\boldsymbol{k}) = \epsilon_{\nu,+}(-\boldsymbol{k}) = \epsilon_{\nu,-}(\boldsymbol{k})$ at all $\boldsymbol{k}$.

In contrast, if the crystal lacks the inversion symmetry, then the degeneracy of the single-electron bands $\epsilon_n(\boldsymbol{k})$ is lifted everywhere, except from some points or lines of high symmetry. In particular, the bands always touch at $\boldsymbol{k} = \mathbf{0}$ (the Γ point), because of the Kramers theorem: time-reversal symmetry means that $|\boldsymbol{k},n\rangle$ and $K|\boldsymbol{k},n\rangle \sim |-\boldsymbol{k},n\rangle$ have the same energy. In the case of $CePt_3Si$, one can show that the spin-split bands touch along the ΓZ line (i.e. along the [001] direction), and there are no other symmetry-imposed degeneracies in the bands crossing the Fermi level (see Sec. III below). In the limit of zero SO coupling (which is not applicable to $CePt_3Si$), but still without an inversion center, the symmetry of the system contains $SU(2)$ spin rotations, in addition to the space group, time reversal, and the gauge group. Then, the bands at each $\boldsymbol{k}$ are double degenerate.

Let us now show that the transformation properties of the single-electron wave functions in the absence of inversion center are different from those of the spin or pseudospin eigenstates, see Eq. (2). Mathematically, the wave functions in each band transform according to irreducible co-representations of the Type II magnetic space group $S_M = S \times \mathcal{K}$ [18] (one should use co-representations because the time-reversal operation K is anti-unitary). In addition, the co-representations must be double-valued because the states $|\boldsymbol{k}\rangle$ are spin-1/2 spinors, so that any rotation by 2π changes their sign: $C_{4z}^4|\boldsymbol{k}\rangle = -|\boldsymbol{k}\rangle$, $\sigma_x^2|\boldsymbol{k}\rangle = -|\boldsymbol{k}\rangle$, and also $K^2|\boldsymbol{k}\rangle = -|\boldsymbol{k}\rangle$ (the band index n is omitted). The double-valuedness can be dealt with in the standard fashion by using the "double-group" trick [19]: one introduces a fictitious new symmetry element $\bar{E}$, which commutes with all other elements and satisfies the conditions $C_{4z}^4 = \sigma_x^2 = \bar{E}$, $\bar{E}^2 = E$, and also $K^2 = \bar{E}$.

The co-representations of S_M can be derived from the usual representations of the unitary component, which in our case coincides with the space group S. For each $\boldsymbol{k}$ in the Brillouin zone, the basis of an irreducible representation of S is formed by the Bloch states corresponding to the star of $\boldsymbol{k}$. The state $K|\boldsymbol{k}\rangle$ belongs to the wave vector $-\boldsymbol{k}$, but the irreducible representations of S corresponding to $\boldsymbol{k}$ and $-\boldsymbol{k}$ are inequivalent (because of the absence of inversion symmetry) and must therefore be regarded as belonging to a single "physically irreducible" representation of twice the dimension [19]. In terms of co-

representations this means that the Bloch states $|\boldsymbol{k}\rangle$ and $K|\boldsymbol{k}\rangle$ belong to the same two-dimensional irreducible co-representation of $S \times \mathcal{K}$ [18]. Thus, the appropriate basis of the Bloch states is formed by the wave functions $|G\boldsymbol{k}\rangle$ corresponding to the star of $\boldsymbol{k}$, and also by their time-reversed counterparts $K|G\boldsymbol{k}\rangle$, which can be combined in a set of bispinors $|\Psi_{\boldsymbol{k}}\rangle = (|\boldsymbol{k}\rangle, K|\boldsymbol{k}\rangle)^T$. All the states from this set have the same energy: $\epsilon(\boldsymbol{k}) = \epsilon(G\boldsymbol{k}) = \epsilon(-\boldsymbol{k})$.

Since the function $G|\boldsymbol{k}\rangle$ belongs to the wave vector $G\boldsymbol{k}$, one can write $G|\boldsymbol{k}\rangle = e^{i\varphi_{\boldsymbol{k}}(G)}|G\boldsymbol{k}\rangle$. The undetermined phase factors come from the freedom in choosing the phases of the Bloch states and realize a representation of the point group in this basis (it is assumed that the Bloch states are single-valued and continuous functions throughout the Brillouin zone). Using the commutation of G and K we have $GK|\boldsymbol{k}\rangle = KG|\boldsymbol{k}\rangle = K\exp[i\varphi_{\boldsymbol{k}}(G)]|G\boldsymbol{k}\rangle = \exp[-i\varphi_{\boldsymbol{k}}(G)]K|G\boldsymbol{k}\rangle$. The co-representation matrices in the basis of bispinor wave functions can be obtained from the relations

$$G|\Psi_{\boldsymbol{k}}\rangle = \begin{pmatrix} e^{i\varphi_{\boldsymbol{k}}(G)} & 0 \\ 0 & e^{-i\varphi_{\boldsymbol{k}}(G)} \end{pmatrix} |\Psi_{G\boldsymbol{k}}\rangle \qquad (3)$$

$$\bar{E}|\Psi_{\boldsymbol{k}}\rangle = \begin{pmatrix} -1 & 0 \\ 0 & -1 \end{pmatrix} |\Psi_{\boldsymbol{k}}\rangle \qquad (4)$$

$$K|\Psi_{\boldsymbol{k}}\rangle = \begin{pmatrix} 0 & 1 \\ -1 & 0 \end{pmatrix} |\Psi_{\boldsymbol{k}}\rangle \qquad (5)$$

[we have taken into account that $K(K|\boldsymbol{k}\rangle) = -|\boldsymbol{k}\rangle$]. Note that the multiplication rules for the co-representation matrices are different from usual unitary group representations. For example, $D(G_1G_2) = D(G_1)D(G_2)$ and $D(GK) = D(G)D(K)$, but $D(KG) = D(K)D^*(G)$ and $D(K^2) = D(K)D^*(K)$ [18].

The general symmetry arguments given above can be illustrated using an exactly-solvable three-dimensional generalization of the Rashba model, which was originally proposed to describe the effects of symmetry lowering near the surface of a semiconductor [20] and recently applied in Refs. [11, 12] to quasi-2D non-centrosymmetric superconductors. Consider a single band $\epsilon_0(\boldsymbol{k})$ in a crystal described by the point group $\mathbf{C}_{4v}$. At zero SO coupling, the band is two-fold degenerate due to spin. The absence of reflection symmetry in the xy plane implies the existence of an internal electric field in the crystal, whose average over a unit cell is non-zero. In the Rashba approximation, this non-uniform field is replaced by its average, introducing a constant vector $\boldsymbol{n} \parallel \hat{z}$. When a non-zero SO coupling is switched on, it can described by an additional term in the Hamiltonian:

$$H_{so} = \alpha \sum_{\boldsymbol{k}} \boldsymbol{n} \cdot (\boldsymbol{\sigma}_{\sigma\sigma'} \times \boldsymbol{k})\, a^\dagger_{\boldsymbol{k},\sigma} a_{\boldsymbol{k},\sigma'}, \qquad (6)$$

where $\sigma, \sigma' = \uparrow, \downarrow$ is the z-axis spin projection, and the states $|\boldsymbol{k}, \sigma\rangle$ are the Bloch spinors at zero SO coupling. Diagonalization of the full single-electron Hamiltonian, $H = H_0 + H_{so}$, gives two bands

$$\epsilon_1(\boldsymbol{k}) = \epsilon_0(\boldsymbol{k}) + \alpha|\boldsymbol{k}_\perp|, \quad \epsilon_2(\boldsymbol{k}) = \epsilon_0(\boldsymbol{k}) - \alpha|\boldsymbol{k}_\perp| \qquad (7)$$

($|\boldsymbol{k}_\perp| = \sqrt{k_x^2 + k_y^2}$), which satisfy the condition $\epsilon_{1,2}(\boldsymbol{k}) = \epsilon_{1,2}(-\boldsymbol{k})$ and additional symmetries from the point group. Also, the bands touch along the line $\boldsymbol{k} \parallel \hat{z}$. It is easy to see that one cannot use pseudospin to label these bands, because the time reversal K transforms the bands into themselves: $|\boldsymbol{k}, n\rangle \to |-\boldsymbol{k}, n\rangle$ $(n = 1, 2)$, while the pseudospin states would be transformed into one another.

To conclude this section, it should be mentioned that the superconductivity in $CePt_3Si$ seems to occur in the presence of anti-ferromagnetic (AFM) order [16], although no data have been reported on the structure of the magnetic phase or the magnitude of the staggered moment. Although the symmetry analysis above was done assuming a paramagnetic normal state, our results can be easily generalized for an AFM case. For a staggered magnetization directed along the z axis, the only change one has to make in the symmetry group is to replace K with $KT_{\boldsymbol{a}}$, which combines the time reversal operation with a lattice translation. Then, Eq. (5) is replaced by

$$KT_{\boldsymbol{a}}|\Psi_{\boldsymbol{k}}\rangle = \begin{pmatrix} 0 & e^{i\boldsymbol{k}\boldsymbol{a}} \\ -e^{-i\boldsymbol{k}\boldsymbol{a}} & 0 \end{pmatrix} |\Psi_{\boldsymbol{k}}\rangle, \qquad (8)$$

so that $(KT_{\boldsymbol{a}})^2|\boldsymbol{k}\rangle = -e^{-2i\boldsymbol{k}\boldsymbol{a}}|\boldsymbol{k}\rangle$.

From the expressions (3)–(8), one obtains the transformation rules for the creation operators of electrons in the Bloch states $|\boldsymbol{k}\rangle$. Although there is some freedom in choosing the phase factors, we will see in Sec. IV that the physically relevant properties are insensitive to the choice of $\varphi_{\boldsymbol{k}}(G)$.

III. ELECTRONIC STRUCTURE

$CePt_3Si$ crystallizes in the same tetragonal structure as $CePt_3B$, with space group P4mm (No. 99). The lattice parameters are $a = 4.072$ Å and $c = 5.442$ Å. Ce is at the 1(b) site (1/2, 1/2, 0.1468), Pt at the 2(c) site (1/2, 0, 0.6504) and at the 1(a) site (0, 0, 0). The z coordinate of the latter site was chosen to be zero. Si is at the 1(a) site (0, 0, 0.4118). These structural parameters all derive from single-crystal x-ray data [16], and can be assumed to be sufficiently accurate for our purposes.

We calculated the electronic structure of $CePt_3Si$ with the full-potential (FP) linear augmented-plane wave (LAPW) method [21, 22, 23], which is based on density functional theory [24]. For the exchange and correlation potential we used the local density approximation [25, 26] (LDA). We performed a non-magnetic calculation, neglecting the AFM order observed experimentally below 2.2 K [16]. The muffin-tin radii of the atoms were chosen as 2.11 a_0. A typical number of plane waves in our basis set was 580. The electronic ground state was calculated self-consistently on a grid of 4212 $\mathbf{k}$ points in the entire Brillouin zone.

For the electronic structure of alloys containing heavy elements, such as Ce and Pt, the SO coupling can in

general not be neglected. In particular, as shown in Sec. IV, for the analysis of the symmetry properties of the superconducting order parameter it is important to obtain an estimate of the SO splitting of the bands near the Fermi energy. The SO coupling has been included in our calculations using the "second variational treatment", as discussed by MacDonald *et al* [27]. In this approach, first the eigenstates are calculated in the absence of the SO interaction. Then, the SO interaction is included in a perturbative way, where the eigenstates up to a certain cut-off energy, calculated without the SO interaction, are used as the basis states. In our calculations this cut-off energy was approximately 22 eV above the Fermi energy.

Although the $CePt_3Si$ structure doesn't have inversion symmetry, the band energies still satisfy the relation $\epsilon_n(\mathbf{k}) = \epsilon_n(-\mathbf{k})$, due to the time reversal symmetry of the single-electron Hamiltonian (see Sec. II). Figure 1 shows the band structure of $CePt_3Si$ without SO coupling calculated along some high symmetry lines. The bands were plotted according to increasing energy. A complete analysis of band crossings based on the character of eigenfunctions was not carried out. However, the bands labeled β and γ do cross between the symmetry points X and M, and so do the β and γ bands between R and A. The γ band and the first dotted band above the Fermi energy have the same symmetry between M and Γ, and hence are unlikely to cross there. The labels of the bands were chosen according to the band index, not the band character, simply to relate various parts of the Fermi surface to the bands crossing the Fermi level. In the electronic density of states (not shown) there is a peak at 0.4 eV above the Fermi energy, which is due to the unfilled Ce-4f electrons. We found that the electrons at the Fermi energy are predominantly of Ce-4f character.

Figure 2 shows the band structure of $CePt_3Si$ with SO coupling [27]. As in Fig. 1 we connected bands with the same band index, ignoring band crossings. In Fig. 2, the bands near the Fermi energy ϵ_F are split by an amount of at most $50 - 200$ meV. This splitting vanishes along the lines $\Gamma - Z$ and $M - A$.

Figure 3 shows the cross sections of the Fermi surface of $CePt_3Si$ in the presence of SO coupling. The splitting of the bands at the Fermi energy due to the SO coupling is prominent in this figure. The sheets of the Fermi surface labeled α and β are hole-like. The γ sheets are electron-like. The α sheet consists of a feature around the Z point. The β band gives rise to a larger feature around the Z point and, in addition, to a feature around the X point [and the symmetry related point $Y = (0, 0.5, 0)$]. The γ bands give rise to a feature around the line $M - A$, which is almost dispersionless in k_z, as well as to a small feature around the Γ point. We further noted that the α bands contribute 1.9% and 3.5% respectively to the density of states at the Fermi energy. Similar contributions coming from the SO split β and γ bands are 25% and 45% and 15% and 9.0%, respectively.

IV. SUPERCONDUCTING ORDER PARAMETER

A. Symmetry analysis

The single-electron states $|\boldsymbol{k}, n\rangle$ can be used as a basis for constructing the Hamiltonian which takes into account the Cooper pairing between electrons. We have $H = H_0 + H_{sc}$, where

$$H_0 = \sum_n \sum_{\boldsymbol{k}} \epsilon_n(\boldsymbol{k}) c^\dagger_{\boldsymbol{k},n} c_{\boldsymbol{k},n}, \tag{9}$$

is the free-electron part, with the chemical potential absorbed into the band energies. As follows from the results of Secs. II and III, the electronic bands $\epsilon_n(\boldsymbol{k})$ are non-degenerate, except along the line $\boldsymbol{k} \parallel \hat{z}$, and invariant under all operations from the point group $\mathbf{C}_{4v}$ and also under inversion: $\epsilon_n(\boldsymbol{k}) = \epsilon_n(-\boldsymbol{k})$. The Fermi surface of $CePt_3Si$ consists of several sheets (see Sec. III), all of which can in principle participate in the formation of the superconducting order.

Assuming a BCS-type mechanism of pairing, the interaction between the band electrons in the Cooper channel can be written in the following form:

$$H_{sc} = H^{(1)}_{sc} + H^{(2)}_{sc} + H^{(3)}_{sc}, \tag{10}$$

where

$$H^{(1)}_{sc} = \frac{1}{2} \sum_n \sum_{\boldsymbol{k},\boldsymbol{k}'} V^{(1)}_n(\boldsymbol{k}, \boldsymbol{k}') c^\dagger_{\boldsymbol{k},n} c^\dagger_{-\boldsymbol{k},n} c_{-\boldsymbol{k}',n} c_{\boldsymbol{k}',n} \tag{11}$$

$$H^{(2)}_{sc} = \frac{1}{2} \sum_{n \neq m} \sum_{\boldsymbol{k},\boldsymbol{k}'} V^{(2)}_{nm}(\boldsymbol{k}, \boldsymbol{k}') c^\dagger_{\boldsymbol{k},n} c^\dagger_{-\boldsymbol{k},n} c_{-\boldsymbol{k}',m} c_{\boldsymbol{k}',m} \tag{12}$$

$$H^{(3)}_{sc} = \frac{1}{2} \sum_{n \neq m} \sum_{\boldsymbol{k},\boldsymbol{k}'} V^{(3)}_{nm}(\boldsymbol{k}, \boldsymbol{k}') c^\dagger_{\boldsymbol{k},n} c^\dagger_{-\boldsymbol{k},m} c_{-\boldsymbol{k}',m} c_{\boldsymbol{k}',n}. \tag{13}$$

The potentials V are non-zero only inside the energy shells of width ω_c (the cutoff energy) near the Fermi surface.

Treating the Cooper interaction between the electrons with opposite momenta in the mean-field approximation, we obtain

$$H_{sc} = \frac{1}{2} \sum_{\boldsymbol{k}} \sum_{nm} \Big[\Delta_{nm}(\boldsymbol{k}) c^\dagger_{\boldsymbol{k},n} c^\dagger_{-\boldsymbol{k},m} + \text{h.c.} \Big]. \tag{14}$$

Here the diagonal matrix elements $\Delta_{nn}(\boldsymbol{k})$ represent the Cooper pairs composed of quasiparticles from the same sheet of the Fermi surface, and the off-diagonal matrix elements $\Delta_{nm}(\boldsymbol{k})$ with $n \neq m$ represent the pairs of quasiparticles from different sheets. From the anti-commutation of the fermionic operators, it follows that $\Delta_{nn}(\boldsymbol{k})$ are odd functions of $\boldsymbol{k}$, but $\Delta_{nm}(\boldsymbol{k}) = -\Delta_{mn}(-\boldsymbol{k})$ with $n \neq m$ do not have a definite parity.

A considerable simplification occurs if to assume that the superconducting gaps are much smaller than the interband energies. The band structure calculations of Sec. III show that typically the SO band splitting E_{so} is of the order of $50-200$ meV (between the bands derived from the degenerate spin-up and spin-down bands at zero SO coupling), which exceeds the superconducting gap by orders of magnitude. In this situation, the formation of interband pairs is energetically unfavorable, and the amplitudes Δ_{nm} with $n \neq m$ vanish. The origin of the suppression of these types of pairing is similar to the well-known paramagnetic limit of singlet superconductivity [28]: the interband splitting E_{so} cuts off the logarithmic singularity in the Cooper channel, thus reducing the critical temperature. Although the condition $E_{so} \gg T_c$ is violated very close to the poles of the Fermi surface where the spin-split bands touch, the off-diagonal Cooper pairing in the vicinity of these points is still suppressed due to the phase space limitations. We also neglect the possibility of the Cooper pairs having a non-zero momentum, i.e. $\langle c^\dagger_{\boldsymbol{k}+\boldsymbol{q},n} c^\dagger_{-\boldsymbol{k},m}\rangle \neq 0$ [Larkin-Ovchinnikov-Fulde-Ferrell (LOFF) phase] [29]. Although the critical temperature of the resulting non-uniform superconducting state can be higher than that of the uniform state, this would not be sufficient to overcome a large depairing effect of the SO band splitting.

Thus, the interband pairing (13) can be neglected, and $\Delta_{nm}(\boldsymbol{k}) = \Delta_n(\boldsymbol{k})\delta_{nm}$ [30]. This is reminiscent of the situation in ferromagnetic superconductors, where only the same-spin components of Δ survive the large exchange band splitting [3]. It follows from Eqs. (3)–(5) and antilinearity of K that

$$
\begin{aligned}
&G(c^\dagger_{\boldsymbol{k},n} c^\dagger_{-\boldsymbol{k},n})G^{-1} = c^\dagger_{G\boldsymbol{k},n} c^\dagger_{-G\boldsymbol{k},n} \\
&\bar{E}(c^\dagger_{\boldsymbol{k},n} c^\dagger_{-\boldsymbol{k},n})\bar{E}^{-1} = c^\dagger_{\boldsymbol{k},n} c^\dagger_{-\boldsymbol{k},n} \\
&K(\lambda c^\dagger_{\boldsymbol{k},n} c^\dagger_{-\boldsymbol{k},n})K^{-1} = -\lambda^* c^\dagger_{-\boldsymbol{k},n} c^\dagger_{\boldsymbol{k},n} \\
&= \lambda^* c^\dagger_{\boldsymbol{k},n} c^\dagger_{-\boldsymbol{k},n},
\end{aligned}
$$

where λ is an arbitrary constant. We have the following transformation rules for the order parameter under the elements of $\mathcal{G}$:

$$
\begin{aligned}
&G: \ \Delta_n(\boldsymbol{k}) \to \Delta_n(G^{-1}\boldsymbol{k}), \\
&K: \ \Delta_n(\boldsymbol{k}) \to \Delta^*_n(\boldsymbol{k}).
\end{aligned}
\tag{15}
$$

Thus, the order parameter components transform like scalar functions. There is no need for double groups, since $\bar{E}$ is equivalent to E when acting on Δ. In the case of an AFM normal state, K should be replaced with $KT_{\boldsymbol{a}}$.

The superconducting order parameter on the nth sheet of the Fermi surface transforms according to one of the irreducible representations Γ of the normal state point group $\mathbf{C}_{4v}$. It can be represented in the form

$$
\Delta_{n,\Gamma}(\boldsymbol{k}) = \sum_{i=1}^{d_\Gamma} \eta_{n,i}\phi_{\Gamma,n,i}(\boldsymbol{k}), \tag{16}
$$

where d_Γ is the dimension of Γ, $\phi_{\Gamma,n,i}(\boldsymbol{k})$ are the basis functions (which are different on different sheets of the Fermi surface in general), and $\eta_{n,i}$ are the order parameter components that enter, e.g., the GL free energy and can depend on coordinates [6]. Despite the absence of inversion center in the crystal, the order parameters Δ_n have a definite parity, namely they are all odd with respect to $\boldsymbol{k} \to -\boldsymbol{k}$. The odd irreducible representations of $\mathbf{C}_{4v}$ are listed in Table I. Since $d_\Gamma = 1$ or 2, the order parameter in each band can have one or two components.

If we neglect the interband pairing described by $H^{(2)}_{sc}$, see Eq. (12), then the order parameters Δ_n are completely decoupled, in particular, they all have different critical temperatures $T_{c,n}$. However, there is no reason to expect these interband terms to be small. If they are taken into account, then all $\Delta_n(\boldsymbol{k})$ are non-zero, so the superconductivity will be induced simultaneously on all sheets of the Fermi surface. The simplest way to see how this works is to use the GL free energy functional, which contains all possible uniform and gradient terms invariant with respect to $\mathcal{G}$. For a one-dimensional representation Γ (the generalization for two-dimensional representations is straightforward), we obtain the following expression for the uniform terms in the free energy density:

$$
F_{uniform} = \sum_{n,m} A_{nm}(T)\eta^*_n\eta_m + F_4, \tag{17}
$$

where F_4 stands for the terms of fourth order (and higher), and A_{ij} is a real symmetric matrix. The off-diagonal elements of A correspond to the interband pairing. The critical temperature T_c is defined as the maximum temperature at which A ceases to be positive definite. Below T_c all η_n are non-zero and proportional to a single complex number η, such that $\eta_n = \varepsilon_n\eta$, where ε_n are constants that can be found by minimizing $F_{uniform}$. Therefore, the components of a one-dimensional order parameter corresponding to the representation Γ are given by

$$
\Delta_n(\boldsymbol{k}) = \eta\varepsilon_n\phi_{\Gamma,n}(\boldsymbol{k}). \tag{18}
$$

Although the basis functions ϕ are different in general, they all have the same symmetry.

Our phenomenological theory cannot determine which pairing channel corresponds to the highest critical temperature. In a recent work, Frigeri *et al* [31] proposed a microscopic model for superconductivity in a noncentrosymmetric crystal, treating the SO coupling as a perturbation with a Rashba-type Hamiltonian. Assuming a strong interband pairing interaction which induces order parameters of the same amplitude on both sheets of the Fermi surface [see Eq. (7)], they predicted a certain gap symmetry for $CePt_3Si$, which seems to correspond to the two-dimensional E representation in our classification.

TABLE I: The character table and the examples of the odd basis functions for the irreducible representations of $\mathbf{C}_{4v}$.

Γ	E	C_{4z}	σ_x	$\phi_\Gamma(\boldsymbol{k})$
A_1	1	1	1	k_z
A_2	1	1	-1	$(k_x^2-k_y^2)k_xk_yk_z$
B_1	1	-1	1	$(k_x^2-k_y^2)k_z$
B_2	1	-1	-1	$k_xk_yk_z$
E	2	0	0	k_x , k_y

B. Gap zeros

The symmetry considerations can help find the zeros in the energy spectrum of Bogoliubov quasiparticles, which are responsible for peculiarities in the low-temperature behavior of unconventional superconductors [6]. The gap structure of the order parameter belonging to the two-dimensional representation E of $\mathbf{C}_{4v}$ depends on the superconducting phase, i.e. on the values of the components η_1 and η_2, which in turn are determined by minimizing the free energy of the superconductor. In contrast, the gap nodes for the one-dimensional order parameters are required by symmetry. Although the momentum dependence of the order parameter is different on different sheets of the Fermi surface, see Eq. (18), the locations of symmetry-imposed gap zeros are the same.

One can easily show that the order parameter corresponding to A_1 vanishes on the plane $k_z = 0$, so that the energy gap has lines of nodes at the equators of all sheets of the Fermi surface. Indeed,

$$\begin{aligned} C_{2z}\phi_{A_1}(\boldsymbol{k}) &= \phi_{A_1}(-k_x,-k_y,k_z) \\ &= \phi_{A_1}(\boldsymbol{k}) = -\phi_{A_1}(-\boldsymbol{k}), \end{aligned} \tag{19}$$

therefore, $\phi_{A_1}(k_x,k_y,0) = 0$. In a similar fashion, one can prove the existence of lines of zeros at $k_z = 0$ for all other one-dimensional representations. Also, the basis functions of A_2 and B_2 have lines of zeros at $k_x = 0$ or $k_y = 0$, while the basis functions of A_2 and B_1 have lines of zeros at $k_x = \pm k_y$. The examples of the basis functions that have only zeros imposed by symmetry are given in Table I.

From the results of Sec. III it follows that some of the sheets of the Fermi surface cross the boundaries of the Brillouin zone. As seen from Eq. (19), the order parameters corresponding to all one-dimensional representations vanish at $k_z = \pm\pi/c$, i.e. at the top and bottom surfaces of the Brillouin zone, because $(k_x,k_y,\pi/c)$ and $(k_x,k_y,-\pi/c)$ are equivalent points. In addition, for the same reason the basis functions of A_2 and B_2 have lines of zeros at $k_x = \pm\pi/a$ or $k_y = \pm\pi/a$.

The gap nodes for one-dimensional order parameters are present at the same locations on all sheets of the Fermi surface and can disappear only if the interband pairing interactions $H_{sc}^{(3)}$, see Eq. (13), are taken into account.

C. Helical superconducting states

In addition to the uniform terms (17), the GL functional for the order parameter corresponding to a one-dimensional representation of $\mathbf{C}_{4v}$ also contains gradient terms

$$\begin{aligned} F_{grad,1} \;=\; \sum_{n,m}\Big[& K^{\perp}_{nm}(\boldsymbol{D}_\perp\eta_n)^*(\boldsymbol{D}_\perp\eta_m) \\ & + K^{z}_{nm}(D_z\eta_n)^*(D_z\eta_m)\Big], \end{aligned} \tag{20}$$

where $\boldsymbol{D} = \boldsymbol{\nabla} + i(2\pi/\Phi_0)\boldsymbol{A}$, $\Phi_0 = \pi\hbar c/e$ is the flux quantum, $\boldsymbol{A}$ is the vector potential, and $\boldsymbol{D}_\perp = (D_x, D_y)$. The coefficients $K^{\perp}_{nm}$ and K^{z}_{nm} are real symmetric matrices. The terms (20), which are of the second order in $\boldsymbol{D}$, are present in any multi-band tetragonal superconductor with the order parameter corresponding to a one-dimensional representation of the symmetry group. However, in the absence of an inversion center, one can have additional terms in the GL functional, which satisfy all the necessary symmetry requirements but are of the first order in gradients [15]. In our case, they can be written in the form

$$F_{grad,2} = \sum_{n,m} L_{nm}(\eta_n^* D_z\eta_m - \eta_m^* D_z\eta_n), \tag{21}$$

where L_{nm} is a real anti-symmetric matrix, which is non-zero only if the interband pairing (12) is present. The terms (21) lead to the possibility that the superconducting state which appears immediately below T_c can be non-uniform, even without external magnetic field.

Consider for simplicity only two bands participating in superconductivity, i.e. $n = 1, 2$. In this case, the matrix L in Eq. (21) has only one non-zero element: $L_{12} = -L_{21} = \lambda/2$. The critical temperature for the superconducting state

$$\eta_1(\boldsymbol{r}) = \eta_{1,0}e^{iqz}, \quad \eta_2(\boldsymbol{r}) = \eta_{2,0}e^{iqz} \tag{22}$$

is determined by the stability condition of the quadratic terms (both uniform and gradient) in the GL functional towards formation of a state with non-zero $\eta_{n,0}$. From Eqs. (17,20,21), one has the following equation for $T_c(q)$:

$$\det\begin{vmatrix} A_{11}+K_{11}q^2 & A_{12}+K_{12}q^2+i\lambda q \\ A_{12}+K_{12}q^2-i\lambda q & A_{22}+K_{22}q^2 \end{vmatrix} = 0, \tag{23}$$

where $A_{11}(T) = a_1(T-T_1)$ and $A_{22}(T) = a_2(T-T_2)$, with T_1 and T_2 having the meaning of the critical temperatures for the bands 1 and 2 respectively in the absence of any interband coupling. The phase transition temperature is obtained by the maximization of $T_c(q)$ with respect to q. It is easy to show that the maximum critical temperature corresponds to a state with $q \neq 0$ (a "helical" state [15]) if the following condition is satisfied:

$$\lambda^2 + 2A_{12}K_{12} - A_{11}(T_{c,0})K_{22} - A_{22}(T_{c,0})K_{11} > 0, \tag{24}$$

where $T_{c,0} = T_c(q = 0)$. However, even if this condition is violated and the phase transition occurs from the normal state to a uniform superconducting state, there remains a possibility that this uniform state becomes unstable towards the formation of a helical state at a lower temperature. To find this instability, one has to include non-linear terms in the free energy. Because of a large number of the phenomenological parameters in the GL functional with the higher-order terms, the phase diagram of this system is quite rich [15]. In particular, there exist various types of helical phases with $q \neq 0$, separated from one another and from the uniform phase by additional phase transitions below T_c.

It should be emphasized that the origin of the helical superconducting states is different from that of the LOFF non-uniform states [29]. In terms of the GL functional, the LOFF state corresponds to the sign change of the second-order gradient term at some values of the parameters (e.g. of the external magnetic field), while our helical instability occurs because of the presence of the first-order gradient terms.

V. CONCLUSION

We have shown that the order parameter in a non-centrosymmetric superconductor with strong spin-orbit coupling has only intra-band components and is always odd with respect to $\boldsymbol{k} \to -\boldsymbol{k}$, which is a consequence of Pauli principle. This should be contrasted to the case of zero spin-orbit coupling, in which the bands are two-fold degenerate. In that limit, one cannot separate the odd and even components of Δ because of the lack of inversion symmetry, so the order parameter does not have a definite parity.

The Fermi surface of $CePt_3Si$ consists of three pairs of sheets, α, β, and γ, each split by the spin-orbit coupling. Our band structure calculations reveal that the states at the Fermi level are predominantly of Ce-4f character. These states are affected strongly by spin-orbit coupling, which leads to the band splitting energy as high as $50 - 200$ meV. The splitting vanishes along the Γ – Z and A – M symmetry lines. By far the biggest contribution to the density of states at the Fermi level comes from the β sheets.

Although the large value of the spin-orbit band splitting excludes the superconducting states that correspond to the pairing of electrons from different sheets of the Fermi surface, one can expect that the interband pair scattering will induce gaps of the same symmetry on all sheets of the Fermi surface. Possible gap structure of $CePt_3Si$ depends on the dimensionality of the order parameter. If the order parameter corresponds to a one-dimensional representation of the group $\mathbf{C}_{4v}$, then the gap has line nodes where the Fermi surface crosses the high-symmetry planes or the boundaries of the Brillouin zone: at $k_z = 0, \pm\pi/c$ for all 1D representations; at $k_x = 0, \pm\pi/a$ and $k_y = 0, \pm\pi/a$ for A_2 and B_2; at $k_x = \pm k_y$ for A_2 and B_1.

The presence of the gap nodes would manifest itself, e.g. in a power-law behavior of thermodynamic and transport characteristics at $T \to 0$. Although the gap symmetries on all sheets of the Fermi surface should be the same, their magnitudes may be different. The experimental data, e.g. a reduced value of the specific heat jump at T_c [16], indicate that only some parts of the Fermi surface have non-zero superconducting gaps, while others remain normal. If this is indeed the case, then the specific heat would drop as $C(T)/T \propto \text{const} + aT$ at low temperatures (with the constant contribution coming from the normal sheets of the Fermi surface), which seems to agree with the experimental data of Ref. [16] in zero field. More detailed information about the pairing symmetry can be obtained only if the precise location of the line nodes is known.

The absence of inversion symmetry can also have interesting consequences for the spatial structure of the superconducting phase. We showed that, in contrast to the centrosymmetric case, the Ginzburg-Landau free energy can now contain additional terms which are of the first order in gradients. Such terms can make the superconducting phase unstable towards the formation of a non-uniform (helical) state even at zero magnetic field. For the order parameters corresponding to the one-dimensional representations of $\mathbf{C}_{4v}$, this possibility exists only if the interband pairing is taken into account.

Acknowledgements

The authors thank B. Mitrovic for useful discussions, and also D. Agterberg, E. Bauer, and especially V. Mineev for stimulating correspondence. This work was supported by the Natural Sciences and Engineering Research Council of Canada.

[1] G. E. Volovik and L. P. Gor'kov, Sov. Phys. JETP **61**, 843 (1985) [Zh. Eksp. Teor. Fiz. **88**, 1412 (1985)].
[2] K. Ueda and T. M. Rice, Phys. Rev. B **31**, 7114 (1985).
[3] K. V. Samokhin and M. B. Walker, Phys. Rev. B **66**, 024512 (2002); K. V. Samokhin and M. B. Walker, Phys. Rev. B **66**, 174501 (2002); K. V. Samokhin, Phys. Rev. B **66**, 212509 (2002).
[4] I. A. Fomin, JETP Lett. **74**, 111 (2001) [Pis'ma Zh. Eksp. Teor. Fiz. **74**, 116 (2001)]; I. A. Fomin, JETP **95**, 940 (2002) [Zh. Eksp. Teor. Fiz. **122**, 1089 (2002)].
[5] V. P. Mineev, Phys. Rev. B **66**, 134504 (2002); V. P. Mineev, T. Champel, preprint cond-mat/0306471, to be published in Phys. Rev. B.
[6] V. P. Mineev and K. V. Samokhin, *Introduction to*

Unconventional Superconductivity (Gordon and Breach, London, 1999).
[7] P. W. Anderson and E. I. Blount, Phys. Rev. Lett. **14**, 217 (1965).
[8] A. C. Lawson and W. H. Zachariasen, Phys. Lett. **38A**, 1 (1972).
[9] J. F. Schooley, W. R. Hosler, and M. L. Cohen, Phys. Rev. Lett. **12**, 474 (1964).
[10] V. V. Bogatko and Yu. N. Venevtsev, Sov. Phys. Solid State **25**, 859 (1983) [Fiz. Tverd. Tela **25**, 1495 (1983)].
[11] V. M. Edelstein, JETP **68**, 1244 (1989) [Zh. Eksp. Teor. Fiz. **95**, 2151 (1989)]; V. M. Edelstein, Phys. Rev. Lett. **75**, 2004 (1995).
[12] L. P. Gor'kov and E. I. Rashba, Phys. Rev. Lett. **87**, 037004 (2001).
[13] V. Barzykin and L. P. Gor'kov, Phys. Rev. Lett. **89**, 227002 (2002).
[14] L. S. Levitov, Yu. V. Nazarov, and G. M. Eliashberg, JETP Lett. **41**, 445 (1985) [Pis'ma Zh. Eksp. Teor. Fiz. **41**, 365 (1985)].
[15] V. P. Mineev and K. V. Samokhin, JETP **78**, 401 (1994) [Zh. Eksp. Teor. Fiz. **105**, 747 (1994)].
[16] E. Bauer, G. Hilscher, H. Michor, Ch. Paul, E. W. Scheidt, A. Gribanov, Yu. Seropegin, H. Noël, M. Sigrist, and P. Rogl, Phys. Rev. Lett. **92**, 027003 (2004).
[17] V. P. Mineev, JETP Lett. **57**, 680 (1993) [Pis'ma Zh. Eksp. Teor. Fiz. **57**, 659 (1993)].
[18] E. Wigner, *Group Theory and Its Applications to the Quantum Mechanics of Atomic Spectra* (Academic Press, NY, 1959); C. J. Bradley and B. L. Davies, Rev. Mod. Phys. **40**, 359 (1968).
[19] L. D. Landau and E. M. Lifshitz, *Quantum Mechanics*, 3rd Edition (Butterworth-Heinemann, Oxford, 2002).
[20] E. I. Rashba, Sov. Phys. Solid State **2**, 1109 (1960).
[21] P. Blaha, K. Schwarz, P. Sorantin, and S. B. Trickey, Comp. Phys. Commun. **59**, 399 (1990).
[22] G. K. H. Madsen, P. Blaha, K. Schwarz, E. Sjöstedt, and L. Nordström, Phys. Rev. B **64**, 195134 (2001).
[23] K. Schwarz, P. Blaha, and G. K. H. Madsen, Comp. Phys. Commun. **147**, 71 (2002).
[24] W. Kohn and L. J. Sham, Phys. Rev. **140**, A1133 (1965).
[25] J. P. Perdew and Y. Wang, Phys. Rev. B **45**, 13244 (1992).
[26] Some trial calculations using the linear muffin-tin orbital method [O. K. Andersen, Phys. Rev. B **12**, 3060 (1975)] produced similar results for the LDA and the generalized gradient approximation [J. P. Perdew, J. A. Chevary, S. H. Vosko, K. A. Jackson, M. R. Pederson, D. J. Singh, and C. Fiolhais, Phys. Rev. B **46**, 6671 (1992)].
[27] A. H. MacDonald, W. E. Pickett, D. D. Koelling, J. Phys. C: Solid St. Phys. **13**, 2675 (1980).
[28] B. S. Chandrasekhar, Appl. Phys. Lett. **1**, 7 (1962); A. M. Clogston, Phys. Rev. Lett. **9**, 266 (1962).
[29] A. I. Larkin and Yu. N. Ovchinnikov, Sov. Phys. JETP **20**, 762 (1965) [Zh. Eksp. Teor. Fiz. **47**, 1136 (1964)]; P. Fulde and R. A. Ferrell, Phys. Rev. **135**, 550 (1964).
[30] That there is only one type of pairing possible in non-centrosymmetric systems with spin-orbit coupling, was pointed out in P. W. Anderson, Phys. Rev. B **30**, 4000 (1984).
[31] P. Frigeri, D. F. Agterberg, A. Koga, and M. Sigrist, preprint cond-mat/0311354 (unpublished).

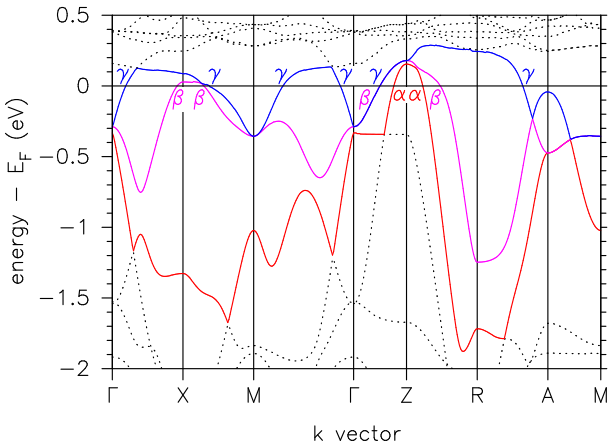


FIG. 1: (Color online) Band structure calculated without SO coupling. Three bands (labeled α, β, and γ) cross the Fermi energy.

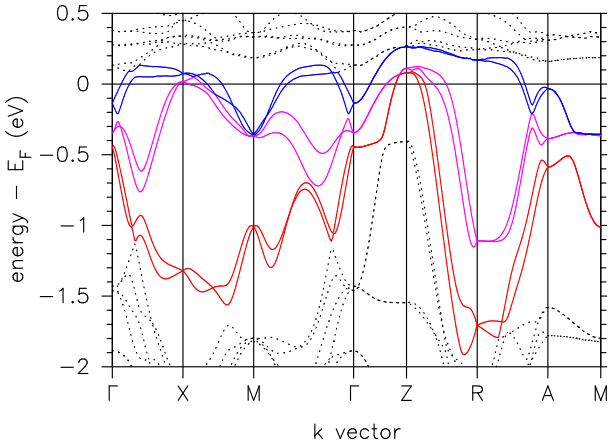


FIG. 2: (Color online) Band structure of $CePt_3Si$ with SO coupling. Bands are split due to the SO interaction (cf. Fig. 1). The bands that cross the Fermi energy, are plotted as solid lines.

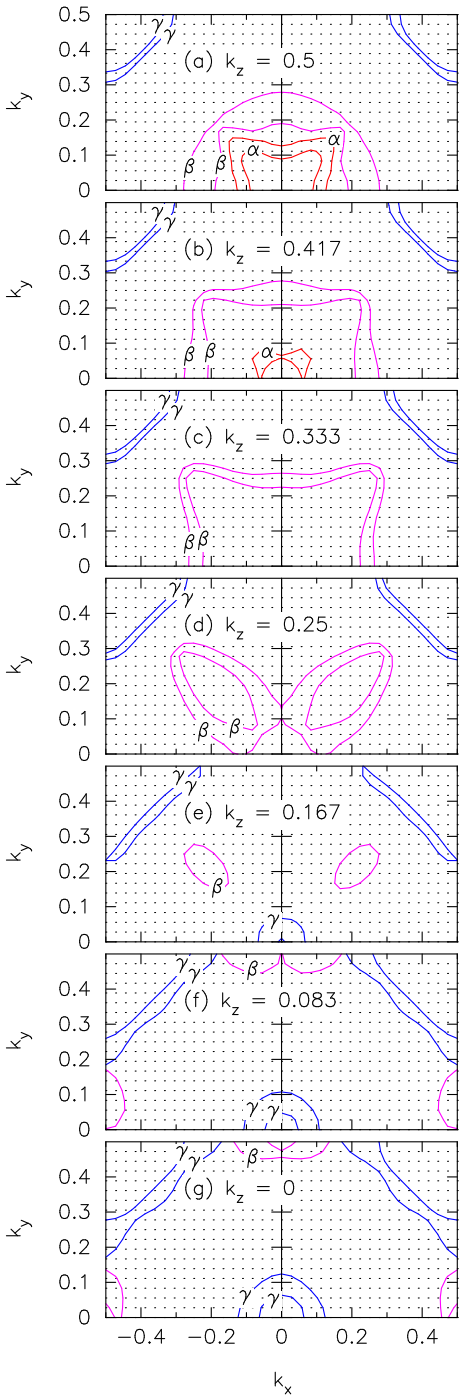


FIG. 3: (Color online) Fermi surface of $CePt_3Si$. The subfigures (a)–(g) show cross sections for different values of k_z (k_z is measured in units of $2\pi/c$, and $k_{x,y}$ are measured in units of $2\pi/a$). Only one quarter of the Brillouin zone is shown. By applying the reflection symmetries in the $k_y = 0$ and $k_z = 0$ planes, the Fermi surface in the entire Brillouin zone can be recovered. The labels of the sheets correspond to the labels in Fig. 1. Dots indicate the **k** points for which we calculated the band energies. The Fermi surface was obtained by interpolating between these points.